Numerical study of bending test on compacted clay by discrete element method: tensile strength determination

A. Ammeri, M. Jamei, M. Bouassida, Olivier Ple, Pascal Villard, J.P. Gourc

Numerical study of bending test on compacted clay by discrete element method: tensile strength determination

A. Ammeri[(a)], M. Jamei[(b)*], M. Bouassida[(a)], O. Plé[(c)*], P. Villard[(c)] , J.P. Gourc[(d)]

[(a)] Geotechnical Engineering Research team, National Engineering School of Tunis (ENIT), Tunisia; [(b)] Civil Engineering Laboratory, National Engineering School of Tunis (ENIT), Tunisia; [(c)] Laboratoire 3S-R, UMR 5521, University Joseph Fourier of Grenoble, France; [(d)] Laboratoire THE, UMR 5564, University Joseph Fourier of Grenoble, France

Abstract: The study of the tensile behaviour of clay is one of the topics which requires a specific lighting especially when one pays a close attention to the pathology of work built with or on clays subjected to significant tensile forces. Therefore, failure or damage of clay, under specific conditions, can be related to tensile stress limit and not to shear stress limit. It is the case of compacted clay liners in landfill cap cover subjected to differential settlements within the waste. In order to study the tensile compacted clay behaviour, a series of laboratory bending tests were carried out. The analysis of the results and the determination of relevant parameters are difficult. Extrapolation to mechanical clay behaviour could not be directly obtained. On the basis of the test results, different numerical simulations using Discrete Element Method were performed and compared with an analytical model, which seems to be the most suitable to interpret bending tests results for the clay soils. As main result, the Discrete Element Method confirms that the compression stress remains linear function of the strain during the bending test until the failure. However, the tensile stresses increase as a non-linear function. For the tensile strength determination, the analytical differential model remains efficient only when the tensile strain field is well measured.

Keywords: tensile, bending test, modelling, discrete element method.

[*] Corresponding authors: E-mail: mehrez.jamei@enit.rnu.tn and olivier.ple@ujf-grenoble.fr

1 INTRODUCTION

Implementation of clay liners in landfill cap cover poses many problems. Because of the real presence of compressible waste as foundation, this operation requires to carry out a compaction of weak energy. However, potential differential settlements within the waste should be considered. This phenomenon can induce bending strains in the clay layer and leads to damage once the cracks developed. As the clay barrier is a major element of site safety, the mechanical behaviour of the clay must be investigated both before and after cracking. Despite the fact of several constitutive laws for compression or for shear were proposed in the literature, some aspects of clay behaviour were poorly investigated such as the tensile strength. As experiments are very difficult to conduct under tensile effort, the challenge to set up an efficient protocol which leads to the tensile strength is not completely resolved. For rock or concrete materials, according to many authors (Cai and Kaiser, 2004; Claesson and Bohloli, 2002), it is often necessary to resort to indirect tensile tests (such flat Brazilian test or beam test). Indeed, Kaklis et al., (2005) reported indirect tensile tests are simple to perform.. However, many problems are associated with indirect tensile tests especially when conducted on clay soils, such as the flatten effect in the Brazilian test, in which shear stresses are induced at the vicinity of the loading plate preventing the tensile stresses to develop. Furthermore, preparing a beam of clayey soil with an appropriate twinge, necessary to well predict the bending behaviour, is also a real constraint. Hence, for clayey soils, the theoretical framework classically used to interpret the indirect tensile tests for rock and concrete materials seems to be questioned. Then, in case of brittle materials, the difficulties are essentially related to indirect tests interpretation. Therefore, for materials with ductile behaviour that are used in geotechnical applications, the challenge is even bigger.

An alternative approach is to use the bending beam tests, which is easy to carry out particularly on compact materials. Unfortunately, the results deduced from this test depend on the experimental protocol and on the interpretation method (Satyanarayana and Satyanarayana, 1972). The tensile strength deduced from bending tests depends on the validity of models assumptions. In the literature, three methods were proposed. The first model is the classical elastic beam theory, based on the assumption that the Young's modulus has the same value in tension as in compression (Ajaz and Parry, 1975). The tensile strength is directly obtained using the measurement of applied force during the test. The second model, called the direct method or bi-modular method, keeps the assumption that the stress is proportional to strain, but the value of Young's modulus in tension may differ from that in compression (Ajaz and Parry, 1975). In this method the measurement of the strains in the extreme fibres is required in addition. The constraint related to the using of this method is that the strains should be recorded using special measurement techniques as radiographic or X-rays techniques. Unfortunately these experimental measurements remain difficult to conduct.

The differential method does not assume a preferred stress-strain relationship. The behaviour law is so unknown (Prentis, 1951). Besides, this method has been appeared as an alternative analytical model to interpret the bending tests (Ajaz and Parry, 1975).

A body of research works on clayey soils show that tensile strength deduced from bending test may be higher than that measured by a direct tensile test, the ratio varies between 0.66 and 3 (Berenbaum and Brodie, 1959; Narain and Rawat, 1970; Addanki et al., 1974). For clay Bricks (Hughes et al., 2000) the corresponding beams were 65x65x215 mm and the above ratio was 2.3. For a silty clay (Plasticity Index = 15%, Optimum water content = 22.55%, Maximum dry density = 16.4 KN/m^3), Jack et al. recorded 0.66 as a ratio.

Because of the experimental and theoretical analysis difficulties, alternative numerical technique was developed. The traditional step consists in characterizing the behaviour with experimental data for a phenomenological modelling and then to extend this behaviour to real geotechnical structure thanks to a

numerical simulation (FEM). Unfortunately, the numerical simulations usually used have difficulties in taking into account discontinuities for these materials (especially damage). To get round this difficulty, one can describe the behaviour of the clay by the distinct elements method (DEM). Already developed to model the total behaviour of grains (Cundall and Strack, 1979), this method is not of current use to take into account the cohesive material behaviour. As the soil tested in the study is a silty clay (not a soft soil), the distinct elements method was used. Firstly it was calibrated with the result of Brazilian and unconfined compression tests and then applied to bending beam tests. This paper discusses the validity of the models used to interpret the bending test.

2 A BENDING EXPERIMENTAL PROTOCOL

Experimental tests were carried out at LIRIGM and ENIT laboratories on a silty clay soil coming from a site that is selected for a landfill project (near the city of Nabeul in Tunisia). The physical characteristics of the clayey soil are given in Table 1. Four-points bending tests were selected (Fig. 1) specifically because of constant bending moment in the middle zone of the specimen. Beam tests have been performed on 10 cm x 10 cm x 40 cm samples compacted in an appropriate mould. The distance between the supporting rods must be large enough to limit the influence of the compression zone and to initiate the failure mode under tensile strength (Fig. 1 and Fig. 2). Due to the low twinges of the tested beams, we note that the essential assumptions of beam's theory are not valid. Consequently, numerical and analytical models which are not based on the assumptions of beam's theory were used to interpret the bending experimental results.

Series of experimental quasi-static tests were carried out on unsaturated silty clay. In order to keep the same initial conditions, like the water content and the dry density, the initial water content is fixed to a standard value equal to 2 % higher than the optimum water content (the average of the water content is

17 % ±0.5 %, the degree of saturation is 95%). The dry density is almost the Proctor optimum value and the average of the dry density is 17.3 ±0.3 kN/m^3.

Four displacement transducers were used; two were placed on the support rods, and the others in the middle part of the specimen (Fig. 1). The load was measured by means of a load cell mounted on the upper axial support rods of the press. A constant displacement rate (0.2 mm/mn) was applied through the lower plate of the press. Further, the middle part of the specimen was covered with artificial roughcast made of black and white painting. This part was filmed continuously with a camera (5 million pixel with 1 pixel = 0.11 mm) to monitor the initiation and the progressive propagation of cracks from the bottom to the top of the specimen (Fig. 2).

3 THE DISCRETE ELEMENT APPROACH FRAMEWORK

3.1 Principle of DEM approach

The Discrete Element Method is one of the emerging numerical techniques used to investigate the behaviour of several materials like granular materials. The method consists of a discrete modelling of the material seen like as structure. Each particle (inclusion, aggregate, grain) interacts with its neighbours by simplified laws of interaction. It should be regarded as a "numerical laboratory" intended to characterize the effects of the interactions at different scales. Moreover, by this method it is possible to describe the behaviour of materials beyond the limits imposed by continuum mechanics.

The complexity of the behaviour is taken into account by methods of assembly. Already developed to model the behaviour of grains, this method is not classically used to take into account the cohesive material behaviour. Nevertheless, for clay soils, grains do not correspond to clay particles, but are simply a means to discretize space, and provide appropriate macroscopic mechanical behaviour through a convenient fitting with experimental results. It is worth to note that the granular distribution, the initial

porosity, the shape and the methodology of setting up the particles have also a great influence on the numerical material behaviour.

The main difficulty of DEM is that the parameters needed for the numerical approach are micro-parameters and not macro-parameters as it can be obtained from laboratory tests. Therefore, first steps of computation are needed to fit the micro-parameters with respect to results of basic laboratory tests.

The numerical software used (PFC^{2D}, 1997) is a two dimensional software which is an implementation of the model of Cundall and Strack (1979) based on the principle of molecular dynamics. The algorithm of computation consists in alternating the application of the Newton's second law of motion for particles and force-displacement law for grain contacts. The equations of motion are integrated using an explicit centred finite difference algorithm with a time step Δt .

The basic discrete elements used are discs (2D) of various sizes that interact with each other. It is worth to note that, in order to obtain a more realistic behaviour of soil (particularly to reach high values of internal friction angle), several adjacent particles are jointed together to make clusters.

A cluster is composed of two discs of diameters ratio D/d = 0.6. Clusters were generated with different sizes ranging in the same proportion between D and 2.4D.

In this study, the contact laws are described by five rheological parameters: normal and tangential stiffness (K^n and K^s), maximum normal and shear strengths (C^n and C^s) and friction coefficient (μ). It is assumed the parameters of two particles in contact act in series (Fig. 3).

The stiffness model, in correlation with the elastic behaviour material, is a function of the normal and tangential stiffness. The normal and tangential components of the contact forces (F^n and F^s) are proportional, respectively, to the overlap between two discs in contact and to the tangential displacement at contact.

The corresponding basic equations used to define the contact laws between two particles are:

$$F_i^n(t) = K^n U_i^n(t) \qquad (1)$$

$$\Delta F_i^s = -K^s \Delta U_i^s \quad (2)$$

$$F_i^s(t) = F_i^s(t - \Delta t) + \Delta F_i^s \quad (3)$$

Where F_i^n and F_i^s are respectively the normal and tangential forces at contact (i) between two particles. Also n_i, U_i^n and ΔU_i^s are respectively the normal and relative tangential displacements at contact (i). (Δt) is a time step during the particle movement. The stiffness contact parameters are computed in PFC^{2D} as:

$$K_n = \frac{\left(K_{ni} K_{nj}\right)}{K_{ni} + K_{nj}} \quad (4)$$

$$K_s = \frac{\left(K_{si} K_{sj}\right)}{K_{si} + K_{sj}} \quad (5)$$

Where K_{ni}, K_{nj}, K_{si} and K_{sj} are the stiffness moduli of the particles i and j.The failure behaviour is defined by a Coulomb–like slip model. The adhesion at contact of two particles is defined by normal and tangential local adhesions $C_f{}^n$ and $C_f{}^s$. The adhesions serve to limit the total normal and shear forces that the contact can carry by enforcing adhesion-strength limits. Hence, the tensile and shear strengths, C^n and C^s, of a contact between two particles of diameters d_i and d_j are computed in PFC^{2D} as:

$$C^n = C_f{}^n \min(d_i, d_j) \quad (6)$$

$$C^s = C_f{}^s \min(d_i, d_j) \quad (7)$$

The tangential component of the contact force is limited in magnitude with a Coulomb-like slip model, with friction angle μ. At each step of computation the reliable contacts are re-actualized according to conditions:

$$\left|F^s\right| \geq F_{\max}^s \quad (8)$$

$$F^n \geq C^n \quad (9)$$

$$F^s_{\max} = \max(\mu|F^n|, C^s) \quad (10)$$

The distinct element scheme is based on Newton's second law of motion. Force displacement law at contact for the translational motion and Euler's law for the rotational motion.

$$F_i = m_i(\ddot{x}_i - g_i) \quad (11)$$

$$M_{i(3)} = I_{i(3)}\dot{\omega}_{i(3)} \quad (12)$$

Where m_i is the particle's mass, $\ddot{x}_i$ is its acceleration, g_i is the gravity acceleration of particle (i), $M_{i(3)}$, $I_{i(3)}$ and $\dot{\omega}_{i(3)}$ are respectively the resultant moment, the principal moment of inertia of the particle and the angular acceleration about the principal axis which is normal to the plane of the disc.

If the material behaviour is elastic, the energy supplied to the assembly of particles is conserved. Therefore, it is necessary to introduce a damping term in the equations of motion to obtain a static or a steady-state solution. The local non-viscous damping κ proposed in PFC^{2D} is taken into account substituting equation (11) by:

$$F_i\left(1 - \kappa.sign(V_i)\right) = m_i(\ddot{x}_i - g_i) \quad (13)$$

Where $\kappa.sign(V_i) = \begin{cases} \kappa & if\ V_i \geq 0 \\ -\kappa & if\ V_i < 0 \end{cases}$ and V_i is the particle velocity in the e_i direction.

In this paper, the local damping considered κ = 0.7

The calculation of stress for a discrete system is well established (Bardet, 1998). The average stress tensor can be obtained by (14), (Love, 1927), (Weber, 1966), (Christoffersen et al. 1981), (Cambou et al., 1995)

$$\overline{\overline{\sigma}} = \frac{1}{V}\sum_c \underline{F}^{(c)} \otimes \underline{l}^{(c)} \quad (14)$$

Where $\underline{l}^{(c)}$ is the vector relating the centres of the two particles which are in contact at contact (c), $\underline{F}^{(c)}$ the vector contact forces in (c) and where the sum covers all contacts in the volume (V).

This relationship was introduced first by Love then followed used by many other authors. It can be proved by many ways. Among them, the formulation used in PFC 2D (1997) and proposed by (Thornton and Barnes, 1986). It is based on the main following steps.

The average stress tensor for the volume $V^{(p)}$ occupied by a single particle may be written as

$$\overline{\sigma}_{ij}^{p} = \frac{1}{V^{(p)}} \int_{V^{(p)}} \sigma_{ij}^{(p)} dV^{p} \qquad (15)$$

By applying Gauss theorem integral, one obtains

$$\overline{\sigma}_{ij}^{(p)} = \frac{1}{V^{(p)}} \int_{S^{(p)}} x_i t_i^{(p)} dS^{(p)} \qquad (16)$$

Since each particle is loaded by point forces acting at discrete contact locations

$$\overline{\sigma}_{ij}^{(p)} = -\frac{1}{V^{(p)}} \sum_{N_c} x_i^{(c)} F_j^{(c)} \qquad (17)$$

The minus sign is introduced here to ensure that compressive/tensile forces produce negative/positive average stresses.

The average stress tensor in a volume V containing a large assembly of particles is defined by

$$\overline{\sigma}_{ij} = \frac{1}{V} \int_{V} \sigma_{ij} dV \qquad (18)$$

Since $\sigma_{ij} = 0$ in the voids, the integral can be replaced by a sum over the N_p particles contained within V as

$$\overline{\sigma}_{ij} = \frac{1}{V} \sum_{N_p} \overline{\sigma}_{ij}^{(p)} V^{(p)} \qquad (19)$$

Substituting (17) into(19), we may replace (19) by

$$\bar{\sigma}_{ij} = -\frac{1}{V}\sum_{N_p}\sum_{N_c} x_i^{(c)} F_j^{(c)} \qquad (20)$$

Since measurements are done into circles, and only the particles with centroids that are contained within the measurement circle are considered in the computation of the average stress tensor, a correction factor is introduced in order to take into account the additional area that is being neglected. Finally for an assembly of large and finite number of particles in equilibrium, one obtains

$$\bar{\sigma}_{ij} = -\left(\frac{1-n}{\sum_{N_p} V^{(p)}}\right)\sum_{N_p}\sum_{N_c}\left|x_i^{(c)} - x_i^{(p)}\right| n_i^{(c,p)} F_j^{(c)} \qquad (21)$$

Where the summations are taken over the N_p discs with centroids contained within the measurement circle in the specimen, and over the N_c contacts between discs.

- $\bar{\sigma}_{ij}$ are the average stress components.
- n is the porosity within the measurement circle;
- $V^{(p)}$ is the volume of particle (p), taken to be equal to the area of particle (p) times a unit-thickness;
- $x_i^{(p)}$ and $x_i^{(c)}$ are the locations of a particle centroid and its point of contact, respectively;
- $n_i^{(c,p)}$ is the unit normal vector directed from a particle centroid to its contact location;
- $F_j^{(c)}$ is the force acting at contact (c)

The stress tensor defined by (21) is a useful approximation of the stress tensor used in continuum mechanics for granular assemblies comprising a large but finite number of particles in a circular area (Bathurst and Rothenburg, 1988).

Although the calculation of stress for a discrete system being well defined, different approaches are considered to calculate strain (Catherine et al., 2003). Various methods have been developed to link the DEM and continuum medium approaches to define the strain tensor. As an overview, these methods can

be classified into two groups. The first group, called kinematic homogenization methods, which are based on the spatial discretization, uses interpolation functions of nodal displacement field. Such the case of a graph or a nodal network technique which is constructed by considering the particle centroidal coordinates. Hence, the incremental displacement gradient is calculated by considering the relative incremental displacement along each edge of the graph, and assuming a linear variation of displacement values between adjacent nodes.

Thomas and Bray (1999) and Dedecker et al. (2000) used approaches based on triangulation of the granular medium and displacement of the particle centroids. With the linear variation in displacement assumption, the displacement gradient can be easily calculated. Nevertheless, it appears that the spatial discretization approaches are not suited for problems involving strain localizations because the particle rotations cannot be accounted using these interpolation techniques except some methods proposed by Liao et al. (1997) and Dedecker et al. (2000).

The second group of method includes an energy based method which equates the strain energy in the equivalent continuum to the energy stored in the contacts of discrete elements (Calvetti et al., 1997), (Cambou et al., 2000). It appears these approaches yield to inaccurate estimates of strain.

In this paper, we use the best-fit approach to define local strain (Liao et al. 1997). This approach is based on the translations of individual particles, $u_i^{(p)}$ ($u_i^{(p)}$ means the difference between the translation of particle $'P'$, and the average translation of all particles contained into the measurement circle). The position of particle $'P'$ is denoted $x_i^{(p)}$, ($x_i^{(p)}$ denotes again the difference of the particle position from the average position of all particles contained into the measurement circle). Assuming that every particle would translate according to a deformation gradient tensor α_{ij}, the predicted translations of particles are given by

$$\tilde{u}_i^{(p)} = \alpha_{ij} x_j^{(p)} \qquad (22)$$

A measure of the error in these predicted values is given by

$$e = u_i^{(p)} - \tilde{u}_i^{(p)} \tag{23}$$

Hence, we are looking for that α_{ij} which makes the square-sum of these errors the smallest:

$$F(\alpha_{ij}) = \sum_{N_p} \left| u_i^{(p)} - \alpha_{ij} x_j^{(p)} \right|^2 \tag{24}$$

The condition of minimum error can be written as

$$\frac{\partial F}{\partial \alpha_{ij}} = 0 \tag{25}$$

Substituting (24) into (25) and differentiating, from the following equations the optimum α_{ij} values are obtained.

$$\begin{bmatrix} \sum_{N_p} x_1^{(p)} x_1^{(p)} & \sum_{N_p} x_2^{(p)} x_1^{(p)} \\ \sum_{N_p} x_1^{(p)} x_2^{(p)} & \sum_{N_p} x_2^{(p)} x_2^{(p)} \end{bmatrix} \begin{Bmatrix} \alpha_{i1} \\ \alpha_{i2} \end{Bmatrix} = \begin{Bmatrix} \sum_{N_p} u_i^{(p)} x_1^{(p)} \\ \sum_{N_p} u_i^{(p)} x_2^{(p)} \end{Bmatrix}, i = 1,2 \tag{26}$$

These four equations are solved by performing a single LU-decomposition

Finally the average strain which corresponds to the symmetric part of α_{ij} is deduced.

3.2 The micro-macro relationship in the simulation approach

As mentioned before, the major difficulty in using the DEM for real application is to assign the good micro-properties which lead to global realistic macroscopic behaviour of the studied material.

In order to predict the results of bending tests, the fitting between the micro and macro parameters is done by the comparison between the numerical and the experimental results of two basic laboratory tests: unconfined compression test to fit the stiffness and the compressive failure parameters (Khanal et al., 2005) and indirect tensile test (Brazilian test) to fit the micro mechanical tensile parameters.

To insure the reproducibility of the numerical results, we paid a particular attention to how the particles are set to an initial position in terms of porosity, shapes of cluster and size distributions. For this study, the particles are set to a fixed porosity by a progressive increase in particles' radii with a decrease in the internal friction. The homogeneity of the numerical sample was checked by measuring the porosity in different parts of the testing sample (Fig. 4).

Several numerical simulations were carried out systematically for each of the curve presented. The number of particles used is 18 particles per cm² (5000 to 8000 particles) which is enough to obtain numerical results with dispersion less than 5 %.

Numerical unconfined compression tests were carried out on a rectangular sample of twinge two, and the Brazilian test on a circular sample. In both cases, the loads were applied to the numerical samples by vertically moving two horizontal rigid walls. The vertical velocity is taken small enough to ensure that no influence on the numerical results.

Quantitative results obtained with an initial set of parameters show that the failure mechanism of the clay material is well reproduced by the numerical model (behaviour law, cracking zone and failure mode). Figure 5 shows that the failure mechanisms in experimental and numerical results of unconfined compression tests are identical. The fitting of the micro parameters was done in order to reproduce the whole experimental results. Once the unconfined compression and the Brazilian tests are well reproduced, the micro-parameters retained to fit the experimental results are those given in table 2. Figures 6 and 7 show the results of the numerical prediction of the curves of the experimental tests. Figures 5 and 8 show the numerical and experimental failure mode of the unconfined compression and the Brazilian tests. The experimental curve corresponds to the average tests data.

4 PREDICTING THE BENDING TEST RESULTS

The DEM was used to predict and to analyze the experimental results of the bending tests. The numerical sample is made of 7146 particles positioned according to the numerical procedure described previously. The loading was applied to the beam by vertically moving the upper rods.

The experimental results of the beam tests are presented and compared with the numerical results (Fig. 9). Figure 10 shows similar failure modes. The difference between the x-coordinate failure sections between experimental and numerical tests is not significant while bending moment is constant between the two rods for transferring loads. As shown in Figure 9, the reproducibility of experimental tests is conditioned by the possibility of keeping initial water content and dry density constant. These conditions remain difficult and usually lead to repeat the test several times and to indicate the variability of the results (see above). Nevertheless, the experimental and numerical load-displacement curves are very close.

In order to ensure the convenient failure stress computation, different sections are considered in the area located between the two points for transferring load. The stresses are calculated according formula (21) in measurement circles (Fig. 11). The number of particles included in each circle of measurement is about 50 which makes it possible to obtain a representative value of the average stresses. Figure 12 shows the stress field homogeneity and the independency of the choice of x-coordinate of section in this area.

One of the interests of the numerical study is the possibility to make a fine analysis of the results and to obtain the diagram of normal stresses under different loading (Fig. 13). The numerical diagrams show that there is no equality between stresses in compression and these in tension particularly in extreme fibres (the average stresses are computed in measurement circles). The difference between them increases with the loading rate (maximum of $\sigma_c - \sigma_t = 5\ kPa$). For each load, a non linearity tensile stress diagram is observed. Hence, we conclude that at failure, the compressive stress of clay is higher than the tensile stress. For Troloppe and Chan (1960), non-regular stress-strain behaviour for compacted clay was also observed.

On the other hand the numerical results invalidate the both elastic methods (the classical elasticity theory of the beams and the bimodular elasticity theory), used as models used for the interpretation of the bending tests on low twinge beams of clay soil.

It is also shown (Fig. 13) that the diagram is linear only in compression zone and the corresponding strains remain in elastic domain. However, these diagrams indicate a plastic redistribution of stress in the tension zone.

In that way, the DEM numerical analysis can be used to predict various bending beam tests. Based on the numerical tests, this approach could be used to give an accurate analysis of the different tensile tests. This method can be an interesting tool to help us understanding the mechanical behaviour of clay layers.

5 COMPARISON BETWEEN THE DEM AND ANALYTICAL MODEL

Ajaz and Parry (1975) proposed an alternative suitable analytical model (differential model) to interpret and analyse the bending tests on clay soils. This model does not assume a preferred stress-strain relationship, the behaviour law is unknown

$$\sigma_{c,t} = f(\varepsilon_{c,t}) \tag{27}$$

In each section of beam, we can express the compression and tensile forces F_c and F_t as functions of strains fields (Fig. 14)

$$F_c = \int_0^d b.\sigma_{c,t} dy = \frac{bd}{\varepsilon_c} \int_0^{\varepsilon_c} f(\varepsilon_{c,t}) d\varepsilon_{c,t} \tag{28}$$

$$F_t = \int_{d-h}^0 b\ \sigma_{c,t}\ dy = \frac{b(h-d)}{\varepsilon_t} \int_{\varepsilon_t}^0 f(\varepsilon_{c,t}) d\varepsilon_{c,t} \tag{29}$$

Based on the static equilibrium, we can show that the moment M is given by

$$M = \frac{b\,h^2}{(\varepsilon_c + \varepsilon_t)^2} \int_{\varepsilon_t}^{\varepsilon_c} f(\varepsilon_{c,t})\,\varepsilon_{c,t}\,d\varepsilon_{c,t} \qquad (30)$$

Finally, after differentiating the latter equation with respect to ε_c and ε_t, the model leads to the following non linear system, where the two differential equations are functions of the bending moment which depends on the compression and tensile strains under the form

$$\sigma_c = \frac{1}{\varepsilon_c + \varepsilon_t} \frac{\partial \xi}{\partial \varepsilon_c} \qquad (31)$$

$$\sigma_t = \frac{1}{\varepsilon_c + \varepsilon_t} \frac{\partial \xi}{\partial \varepsilon_t} \qquad (32)$$

Where ξ is given by

$$\xi = \frac{M\left(\varepsilon_c + \varepsilon_t\right)^2}{bh^2} \qquad (33)$$

Hence, the compression and tensile stresses are calculated by differentiating ξ with respect to ε_c and ε_t. It is obvious that the compression and tensile stress values are calculated respectively with the two equations at the top of the bending sample and at its bottom. Only one differentiation is needed to calculate the required values of compression and tensile stresses from experimental values of M, ε_c and ε_t. The authors gave the evolution of the variable term and used a graphical differentiation by drawing tangents at the desired points. Table 3 summarizes the results of numerical and analytical models. The numerical results are the normal stresses at the lower and the upper fibres of the beam deduced from the computed values in the measurement circles (Fig. 11). For the differential method, the process requires the graphical determination of the derivative of ξ function over compression and tensile strain at failure. It appears that the numerical and the differential method give the same qualitative results in the tension zone, but it is not the case for the stress diagram in compression zone (Fig. 13 and Fig. 14). We can also

note that the differential method gives a higher stresses values compared with those obtained by the numerical model. According to several authors (Ajaz and Parry, 1975; Satyanarayana and Satyanarayana, 1972; Ramanathan and Raman, 1975), the ratio between the compression and the tensile stresses varies between 1 and 3 on experimental beam tests. This ratio increases with the increase of water content and becomes more and more sensitive. For our numerical simulations, this ratio is equal to 1.26 for the differential method and equal to 1.11 for the numerical DEM simulation. Due to weak plasticity, the silty clay of Nabeul can be considered close to a brittle material (Fig. 7 and Fig. 9). In that way, we think that the mechanical behaviour of the clay is closer to the numerical DEM results. Despite the restrictions that result from these preliminary results, this shows the importance of using DEM approach for studying the mechanical behaviour of the brittle silty clay of Nabeul.

6 CONCLUSION

The numerical study carried out with the PFC^{2D} code improves the potential of the DEM which can help in predicting many experimental tests. It is shown that the main condition for an efficient use of the DEM is to make a good fitting of micro-parameters from basic convenient experimental tests. Its potentiality depends on the micro-macro calibration.

The analytical differential method is used for comparison because it is not based on a preferred behaviour law assumption. It seems that it leads to the same numerical stress diagram in tension zone. Nevertheless, the tensile strength determined by the differential method is also overestimated comparing with the numerical value (the ratio is 1.2). From the numerical investigation, it is concluded the linear stress-strain relationship in compression zone during the bending test until the failure. While, non-linear tensile stresses are highlighted, especially when failure is approached. This result is relevant of the plastic redistribution of the stress in the tension zone.

Therefore, it appears that the using of the elastic models is not appropriate for this kind of problems and may conduct to an overestimation of the tensile strength. The bending experimental protocol for the kind of material is only used for the low beam twinges. Consequently, the elastic beam theory can not be applied.

On the other hand, the DEM gives a power tool to obtain the tensile stress function of the strain, the cracking development and the failure mode.

Finally, it seems that the contact law presented in this paper is well established for soils with low plasticity (quasi-brittle material). Nevertheless, for materials with high plasticity, another study should be undertaken and another convenient contact law should be implemented.

REFERENCES

Addanki V., Gopala K., Zdenek E. and Nobert R. M. (1974) 'Behaviour of Compacted Soil in Tension', *J. of the Geotechnical Engineering Division*, september, pp.1050-1061.

Ajaz A. and Parry R. H. G. (1975) 'Analysis of bending stresses in soil beams', *Geotechnique*, vol. 25, n°. 3, pp.586-591.

Bardet J-P. (1998) 'Introduction to computational granular mechanics', in *Behaviour of granular materials*, Cambou B.(ed.), No. 385 in CISM Courses and Lectures. Springer: Wien, New York, pp. 99-170.

Bathurst R.J. and Rothenburg L. (1988), 'Micromechanical aspects of isotropic granular assemblies with linear contact interaction', *Journal of Applied Mechanics*, vol. 55, pp. 17-23

Berenbaum R. and Brodie I. (1959) 'Measurement of the tensile strength of brittle materials', *British Journal of Applied Physics*, Vol. 10, pp.281-287.

Cai M. and Kaiser P.K. (2004) 'Numerical simulation of the Brazilian test and the tensile strength of anisotropic rocks with pre-existing cracks', *International Journal of Rock Mechanics & Mining Sciences*, Vol. 41, n°3, pp.1-6.

Calvetti F., Combe G. and Lanier J. (1997), 'Experimental micromechanical analysis of a 2D granular material: relation between structure evolution and loading path', *Mechanics of Cohesive–Frictional Materials*, n°2, pp.121-163.

Cambou B., Chaze M. and Dedecker F. (2000), 'Change of scale in granular materials', *European Journal of Mechanics*, Vol. A(Solids), n° 19, pp. 999-1014.

Cambou B., Dubujet P., Emeriault F. and Sidoroff F. (1995) 'Homogenization for granular materials', *Eur. J. Mech., A/Solids*, vol. 14, n°2, pp. 255-276

Catherine O.S., Jonathan D. B. and Shaofan L. (2003), 'A new approach for calculating strain for particulate media', *Int. J. Numer. Anal. Meth. Geomech.*, n° 27, pp. 859–877

Christoffersen J., Mehrabadi M. M. and Nema-Nasser S. (1981), 'A micromechanical description of granular material behaviour', *J. App. Mech.*, n°48, pp. 339-344.

Claesson J. and Bohloli B. (2002) 'Brazilian test: stress field and tensile strength of anisotropic rocks using an analytical solution', *International Journal of Rock Mechanics & Mining Sciences*, vol. 39, pp.991-1004

Cundall P.A. and Strack O.D.L. (1979) 'A discrete numerical model for granular assemblies', *Geotechnique*, vol. 29(1), pp. 47-65.

Dedecker F., Chaze M., Dubujet P. and Cambou B. (2000), ' Specific features of strain in granular materials', *Mechanics of Cohesive-Frictional Materials*, n° 5, pp. 173-193.

Hughes T.G., Baker M.G. and Harvey R.J. (2000), 'Tensile strengths of masonry components', *Masonry International*, vol. 13, n° 2, pp. 39-43.

Jack A. Harison, Bobby O. Hardin and Kamyar M.(1994) 'Fracture toughness of compacted cohesive soils using ring test', *Journal of Geotechnical Engineering*, vol.120, n° 5, pp. 872-889.

Kaklis K. N., Agioutantis Z., Sarris E. and Pateli A. (2005) 'A theoretical and numerical study of discs with flat edges under diametral compression (Flat Brazilian test)', *5th GRACM International Congress on Computational Mechanics*, Limassol, 29 June-1 July.

Khanal M., Schubert W. and Tomas J. (2005) 'DEM simulation of diametrical compression test on particle compounds', *Granular Matter*, vol. 7, pp.83-90.

Liao C., Chang T., Young D., and Chang C. (1997), 'Stress-strain relationships for granular materials based on the hypothesis of best fit', *International Journal of Solids and Structures*, n°34, pp. 4087-4100.

Love A. E. H. (1927) ' A treatise on the mathematical theory of elasticity'.

Narain J. and Rawat C. (1970): 'Tensile strength of compacted soils'. *J. of the soils Mechanics and Foundations Division*, Vol. 96, n°4, pp.2185-2190.

PFC2D user manual, release 3.00 (1997). Itasca Consulting Group, Inc., Minneapolis.

Prentis H. M. (1951) 'The distribution of concrete stress in reinforced and prestressed concrete beams when tested to destruction by a pure bending moment', *Mag. Conc. Res.*, Vol 2, n° 5, pp. 73-77.

Ramanathan B. and Raman V. (1974) 'Split tensile strength of cohesive soils', *Geotechnical Engineering*, Vol.3, pp.71-75.

Satyanarayana B. and Satyanarayana R. (1972) 'Measurement of tensile strength of compacted soils', Technical note, *Geotechnical Engineering*, Vol. 3, pp. 61-66.

Thomas P.A. and Bray J.D. (1999) 'Capturing the Nonspherical Shape of Granular Media with Disk Clusters', *Journal of Geotechnical and Geoenvironmental Engineering*, n°125(3), pp.169-178.

Thornton C., Barnes D.J. (1986) 'Computer simulated deformation of compact granular assemblies', *Acta Mechanica,* n°64, pp 45-61.

Troloppe D. L. and Chan C. K. (1960) 'Soil structure and step-strain phenomenon', *J. of the soils Mechanics and Foundations Division*, Am. Soc. Civ. Engrs., 86, n°2, pp. 1-39.

Weber J. (1966) 'Recherches concernant les contraintes intergranulaires dans les milieux pulvérulents. Application à la rhéologie de ces milieux', *Cahiers du G.F.R.*, n°3, pp.161-170.

Figure 1: Scheme of beam test in LIRIGM Laboratory

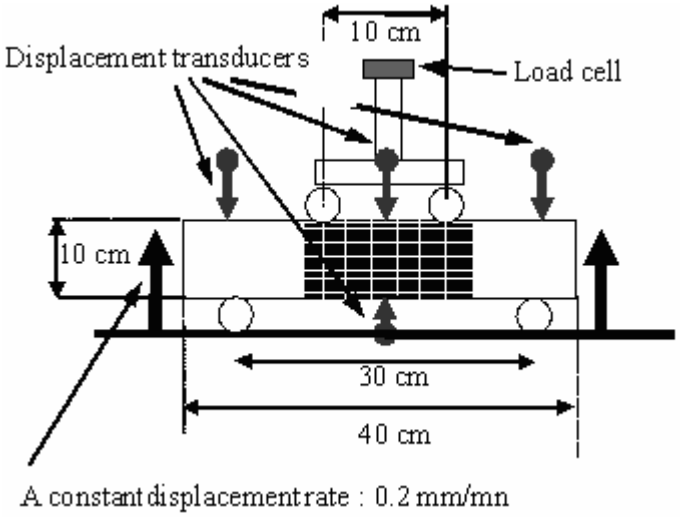

Figure 2: Cracks on the lower part of the beam clay tested in LIRIGM Laboratory

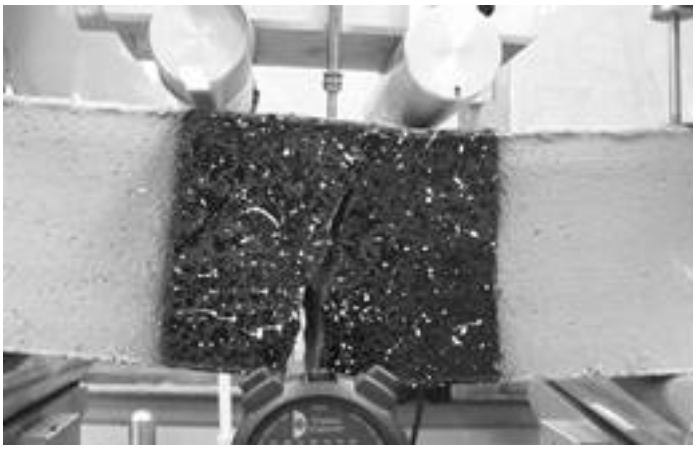

Figure 3: The rheological model of the DEM

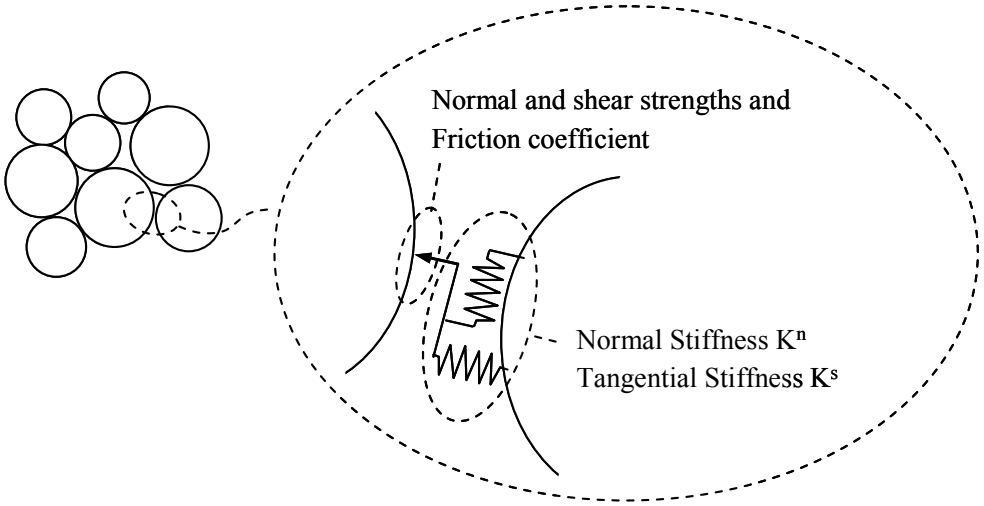

Figure 4: distribution of porosity in the sample

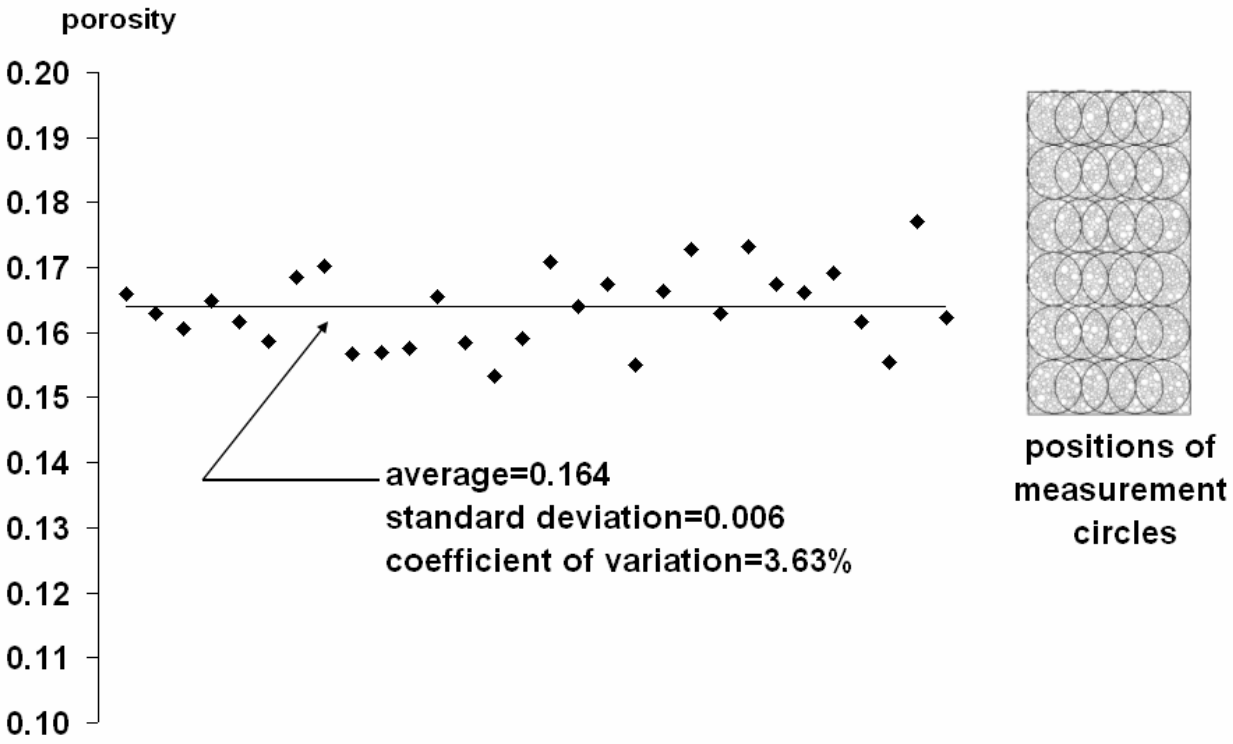

Figure 5: Failure modes in experimental (a) and numerical (b) unconfined compression tests.

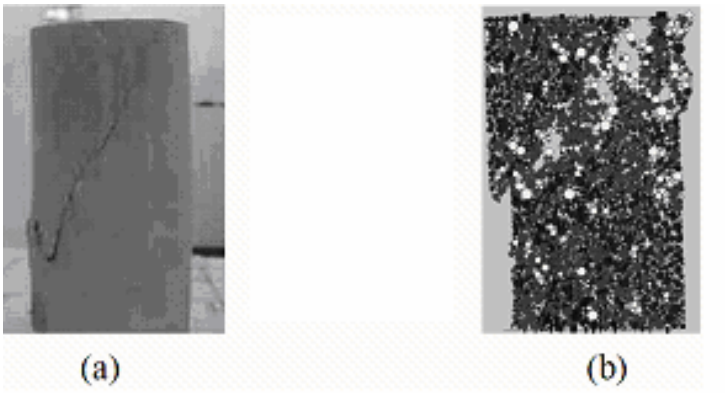

Figure 6: A numerical prediction of unconfined compression test

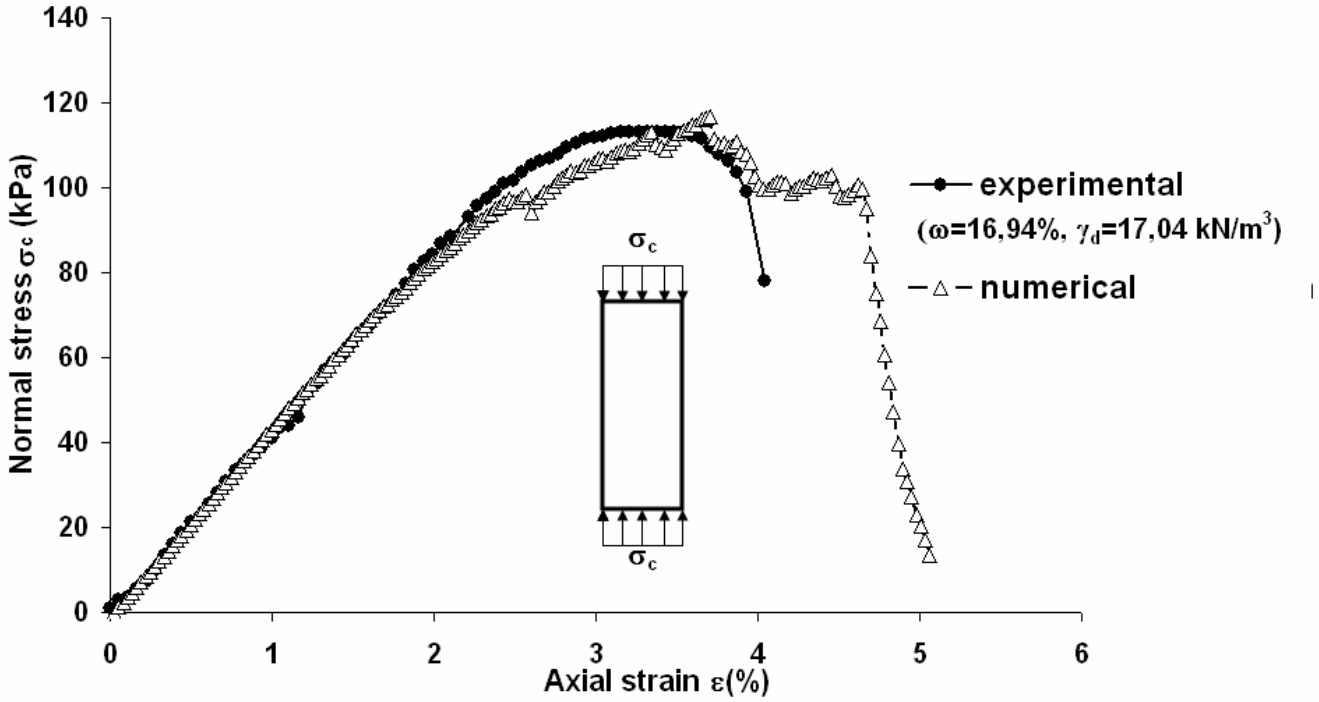

Figure 7: A numerical prediction of the split tensile test

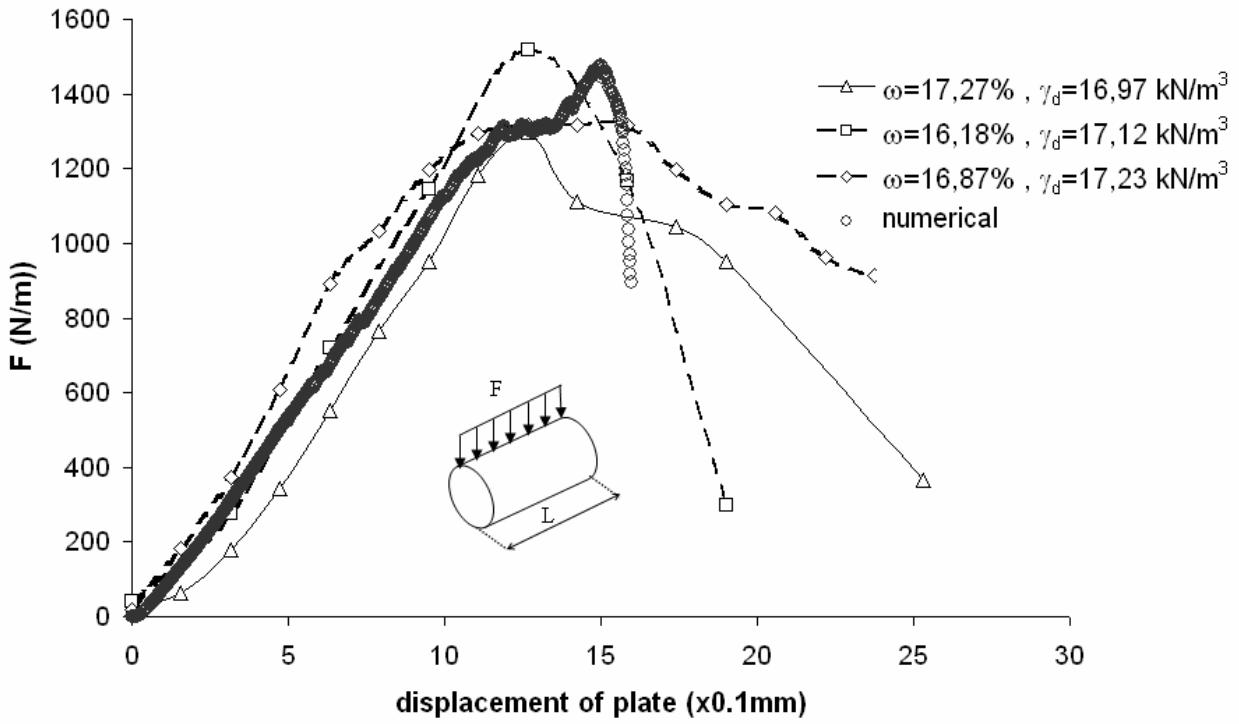

Figure 8: Experimental (a) and numerical (b) Brazilian test failure mode

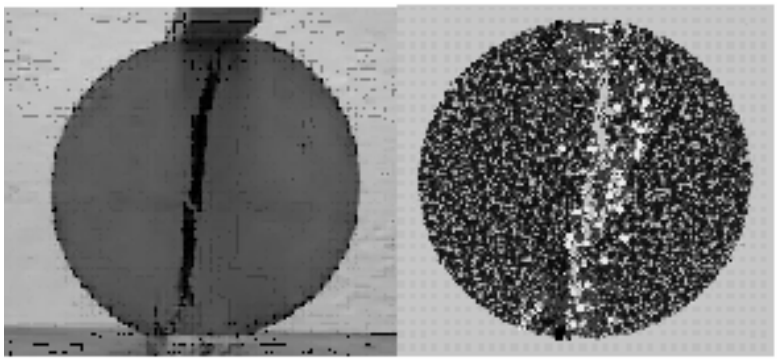

(a) (b)

Figure 9: Experimental and numerical bending tests simulations

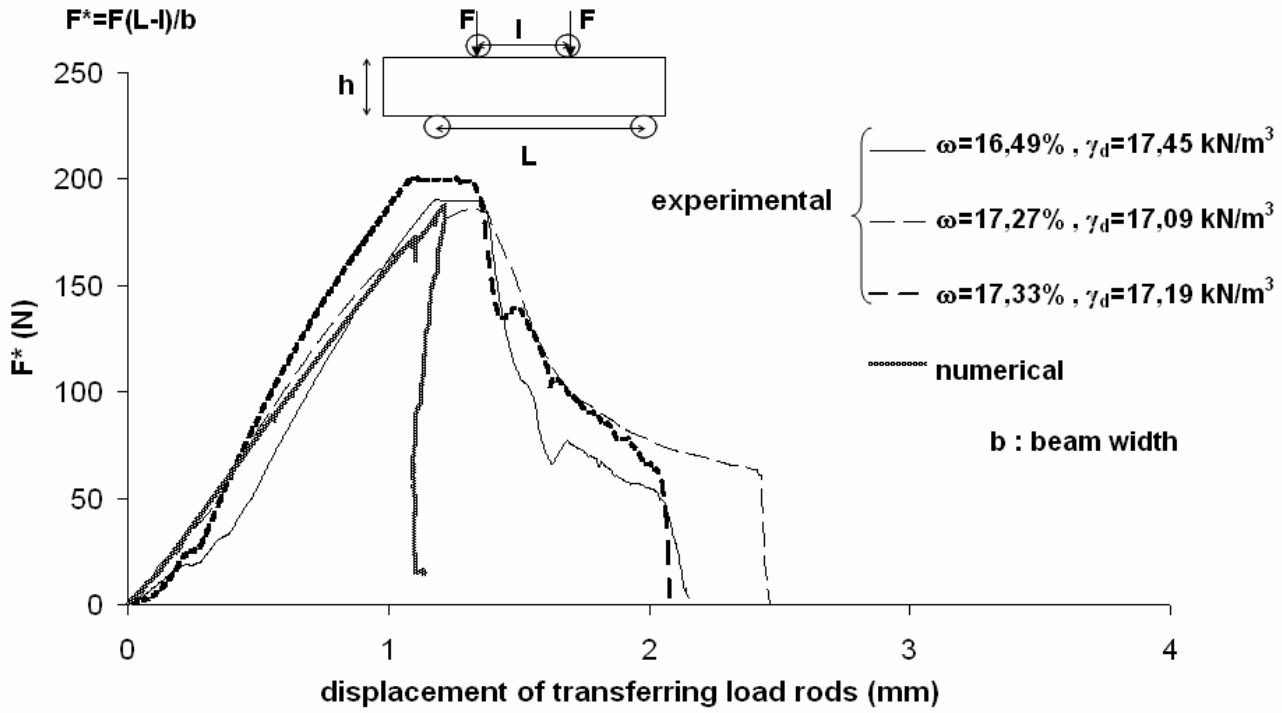

Figure 10: Numerical prediction of failure mode in bending test

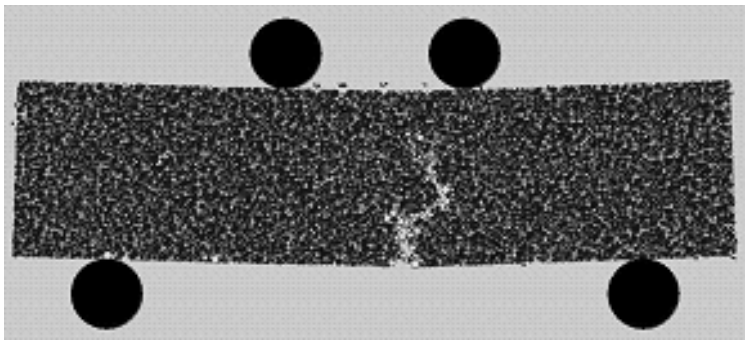

Figure 11: Locations of measurement circles of stress and strain fields

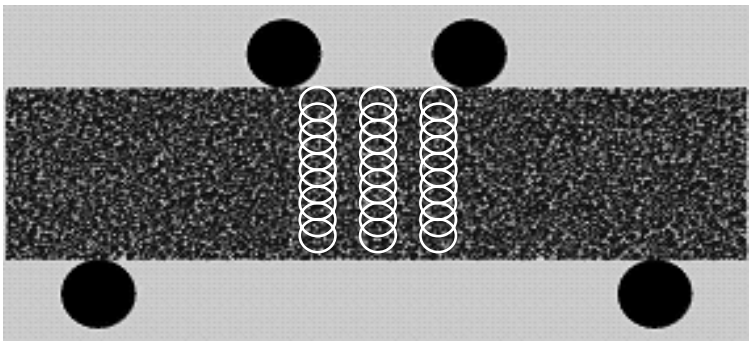

Figure 12: Normal stress curves, at various sections of the beam

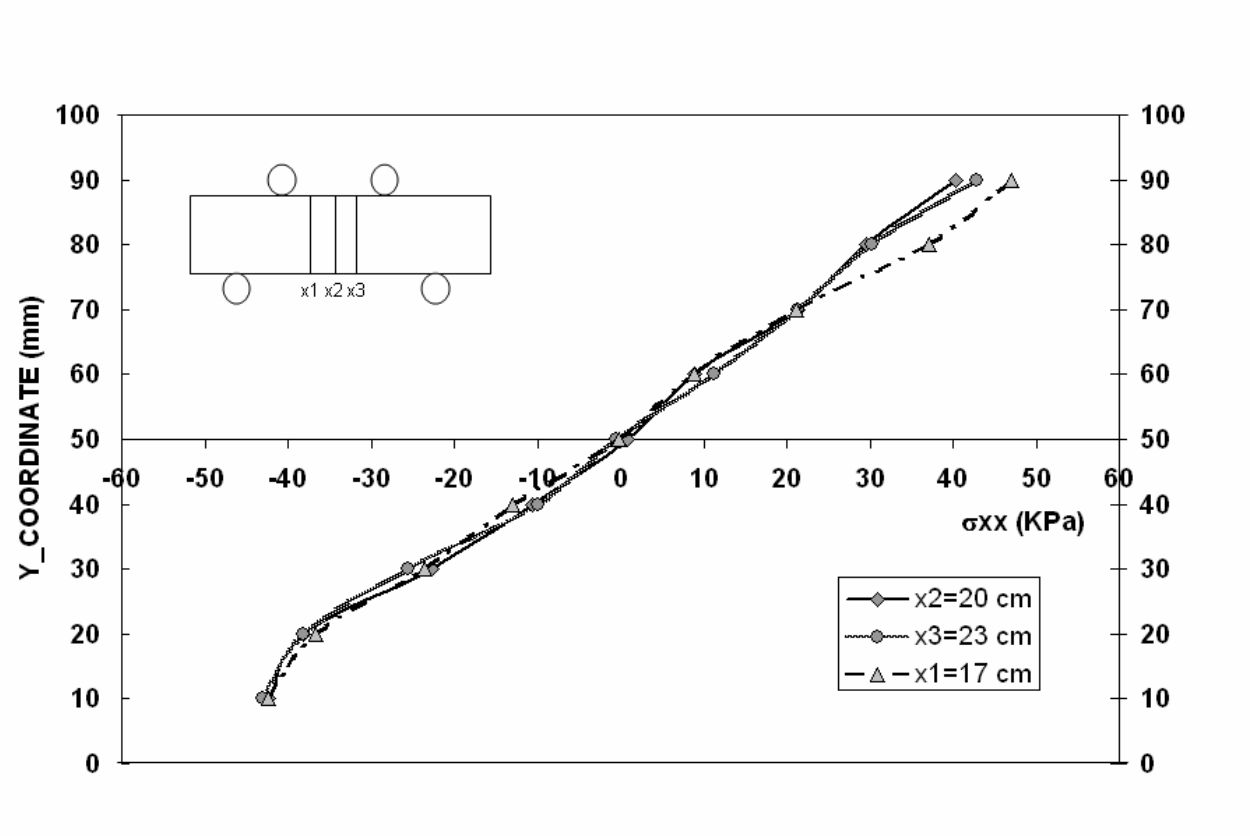

Figure13: Numerical stress curves across medium section at different load (during the test)

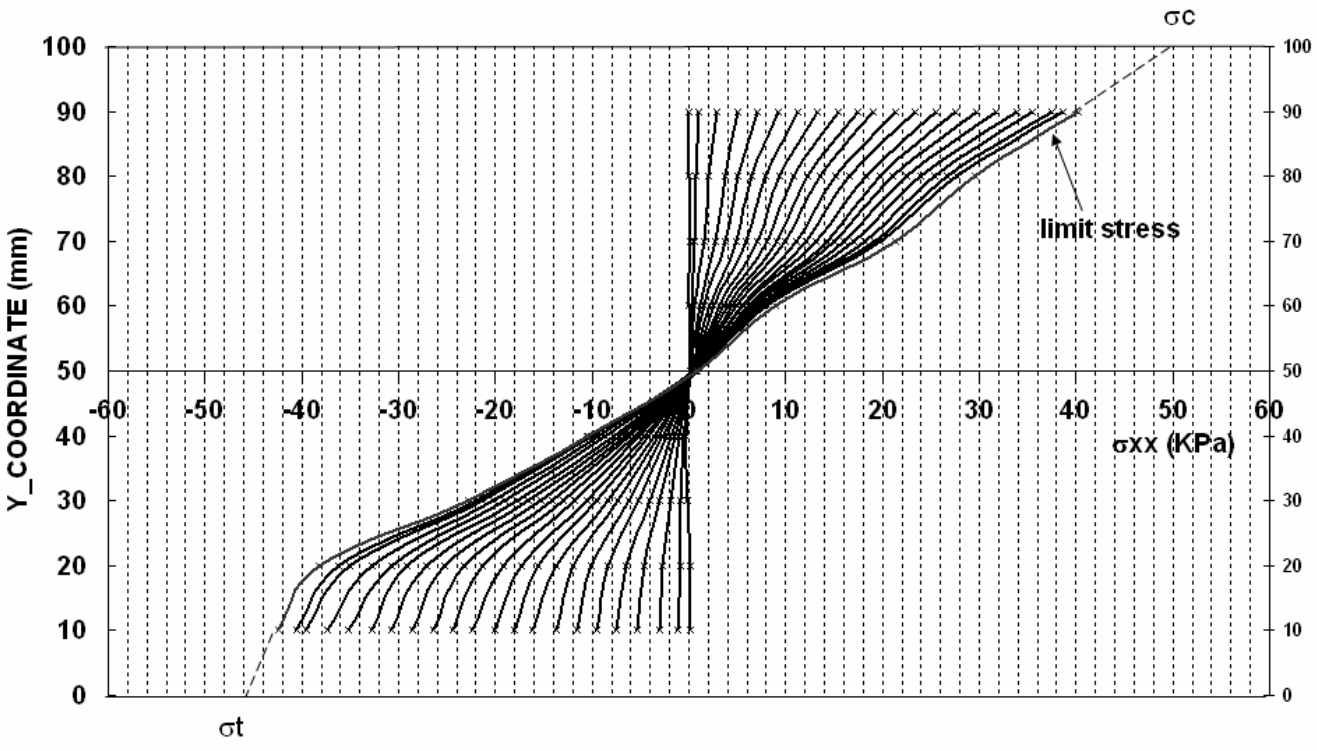

Figure14: Shape of stress diagram for differential method (Ajaz and Parry, 1975)

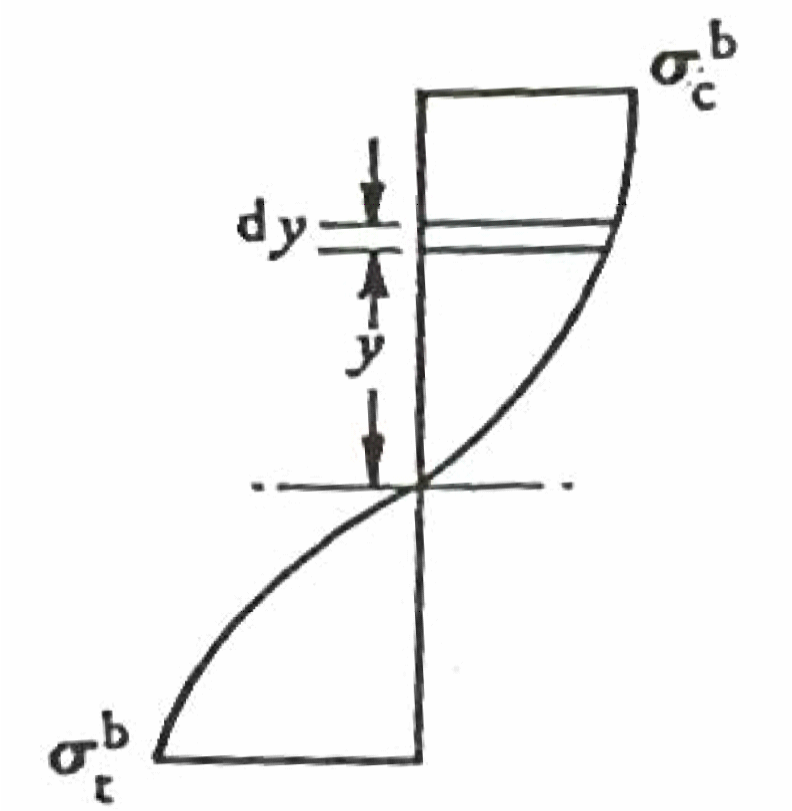

Table 1: Physical and mechanical characteristics of the tested silty clay

Physical and Mechanical Characteristics	
% of size grains < 2 μm	5 %
% of size grain comprising between 2 μm until 80 μm	67 %
Specific density γ_s	26.28 kN/m^3
Void ratio e	0.47
Maximum Dry density (Proctor optimum) γ_{dmax}	17.9 kN/m^3
Optimum water content ω	14.5 %
Plasticity Index PI	13 %
Undrained friction angle ϕ_u	17°
Undrained cohesion C_u	68 kPa

Table 2: Micro-parameters used in the numerical model

Micro-parameters		
k_n	14	MN/m
k_s	14	MN/m
C_f^n	150	kN/m
C_f^s	150	kN/m
μ	0.4	
porosity	0.17	
Density of particles	18	Particles/cm²

Table 3: Compression and tensile stress at failure from different models

	Numerical	Differential method
σ_c(kPa)	50.00	68.34
σ_t(kPa)	45.00	53.95